*polysaccharides*

MDPI

*Article*

# Semi-Synthesis of Chondroitin 6-Phosphate Assisted by Microwave Irradiation

**Fabiana Esposito [1], Sabrina Cuomo [2], Serena Traboni [1], Alfonso Iadonisi [1], Donatella Cimini [3], Annalisa La Gatta [2], Chiara Schiraldi [2] and Emiliano Bedini [1,*]**

[1] Department of Chemical Sciences, University of Naples Federico II, Complesso Universitario Monte S. Angelo, via Cintia 4, I-80126 Naples, Italy; fabiana.esposito3@unina.it (F.E.); serena.traboni@unina.it (S.T.); iadonisi@unina.it (A.I.)

[2] Department of Experimental Medicine, School of Medicine, University of Campania "Luigi Vanvitelli", via L. De Crecchio 7, I-80138 Naples, Italy; sabrina.cuomo@unicampania.it (S.C.); annalisa.lagatta@unicampania.it (A.L.G.); chiara.schiraldi@unicampania.it (C.S.)

[3] Department of Environmental, Biological, and Pharmaceutical Sciences and Technologies, University of Campania "Luigi Vanvitelli", via A. Vivaldi 43, I-81100 Caserta, Italy; donatella.cimini@unicampania.it

* Correspondence: ebedini@unina.it

**Abstract**

Chondroitin sulfate is a glycosaminoglycan polysaccharide, playing key roles in a plethora of physiopathological processes typical of higher animals. The position of sulfate groups within CS disaccharide subunits composing the polysaccharide chain is able to encode specific functional information. In order to expand such a "sulfation code", access to non-natural CS variants and mimics thereof can be pursued. In this context, an interesting topic concerns phosphorylated analogs of CS polysaccharides, as the replacement of sulfate groups with phosphates can lead to unreported activities of phosphorylated CS. In light of this, the phosphorylation reaction of a microbial-sourced, unsulfated chondroitin polysaccharide with phosphoric acid is reported in the present study, testing different microwave irradiation conditions and comparing them with conventional heating procedures. The obtained products were subjected to a detailed characterization, in terms of chemical structure and hydrodynamic properties, by 1D- and 2D-NMR spectroscopy and HP-SEC-TDA analysis, respectively. The characterization study showed how different reaction conditions can not only influence the regioselectivity and degree of phosphorylation but also trigger the formation of phosphate diester functionalities acting as cross-linkers between polysaccharide chains. The results from the screening presented in this work could be interesting for any research devoted to the regioselective phosphorylation of a polysaccharide.

**Keywords:** glycosaminoglycans; chondroitin; phosphorylation; semi-synthesis; microwave irradiation



Academic Editor: Philippe Michaud

Received: 4 November 2025
Revised: 11 December 2025
Accepted: 13 January 2026
Published: 19 January 2026



## 1. Introduction

Chondroitin sulfate (CS) is a glycosaminoglycan (GAG) found in both vertebrates and invertebrates, consisting in a polysaccharide chain composed of disaccharide repeating units made by variously sulfated, alternating β-1⟶3-linked 2-acetamido-2-deoxy-D-galactose (*N*-acetyl-D-galactosamine, GalNAc) and β-1⟶4-linked D-glucuronic acid (GlcA) units [1]. Sulfate groups decorating the CS backbone seem to be a result of evolution, allowing for CS to play key roles in a plethora of physiopathological processes typical of higher animals [2]. It is important to note that their distribution on CS is not only animal-

and tissue-specific, but it also depends on the physiopathological conditions of the single organism, i.e., age, inflammation, tumor formation, etc. [2,3]. The different distributions of sulfate groups within CS disaccharide repeating units are commonly indicated with a letter (Figure 1), and the resulting sequence of sulfated subunits seems to encode specific functional information. Different from other biological codes, such a "sulfation code" is far from being deciphered in detail [4]. Although for a few biological processes, the role of differently sulfated CS variants has been elucidated [5–8], cracking the sulfation code remains elusive due to several factors.

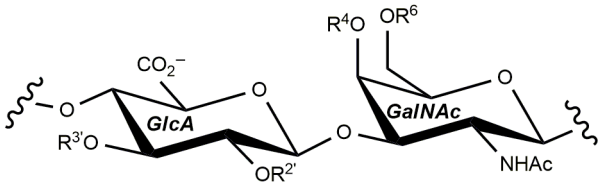


| | R2' | R3' | R4 | R6 | | R2' | R3' | R4 | R6 |
|---|---|---|---|---|---|---|---|---|---|
| 0 | H | H | H | H | M | H | $SO_3^-$ | $SO_3^-$ | $SO_3^-$ |
| A | H | H | $SO_3^-$ | H | R | $SO_3^-$ | $SO_3^-$ | H | H |
| B | $SO_3^-$ | H | $SO_3^-$ | H | S | $SO_3^-$ | $SO_3^-$ | $SO_3^-$ | H |
| C | H | H | H | $SO_3^-$ | S | $SO_3^-$ | $SO_3^-$ | H | $SO_3^-$ |
| D | $SO_3^-$ | H | H | $SO_3^-$ | T | $SO_3^-$ | H | $SO_3^-$ | $SO_3^-$ |
| E | H | H | $SO_3^-$ | $SO_3^-$ | U | $SO_3^-$ | H | H | H |
| K | H | $SO_3^-$ | $SO_3^-$ | H | V | H | $SO_3^-$ | H | H |
| L | H | $SO_3^-$ | H | $SO_3^-$ | | | | | |

**Figure 1.** Sulfation patterns of disaccharide repeating units of CSs (the ones that are most commonly found from animal sources are indicated in red).

Natural CSs are very often composed of two or even more differently sulfated disaccharide subunits, and the identification of their sequence along the polysaccharide backbone is very difficult, having been achieved only in a few simple cases [9–11]. This also makes it very difficult to isolate structurally well-defined CS polysaccharides for structure–activity relationships investigations towards a full deciphering of the CS sulfation code. Nonetheless, to this aim, considerable efforts have been made in recent years through several approaches, spanning from the chemical [12], chemo-enzymatic [13,14], and microbial cell factory synthesis [15,16] of structurally homogeneous CS species to the development of increasingly powerful methods for highly efficient purification [17] and structural characterization of natural CSs [18]. Moreover, some research groups—including ours—are also directing their efforts to try to expand the "sulfation code", i.e., by obtaining non-natural, structurally homogeneous CS variants [19–21] as well as mimics thereof [22]. In this frame, an interesting topic concerns the phosphorylated analogs of CS polysaccharides, because the replacement of sulfate groups with phosphates has been shown by a recent in silico study to lead to unreported activities in phosphorylated CS [23], triggered by the differences in size, polarity, acid–base, and chelation properties between sulfate and phosphate groups [24]. Nonetheless, the preparation of phosphorylated CS and, more generally, phosphorylated GAG species is still rather underdeveloped, with only a few, very recently reported examples [23,25–27]. One of the main reasons is that phosphorylation reactions on common polysaccharides (e.g., cellulose, dextran, alginate) are very often characterized by rather harsh conditions (i.e., heating the reaction mixture to temperatures up to 150 °C), poor yields and degree of phosphorylation (DP), and a lack of control over regiochemistry [28–31].

Surprisingly, to the best of our knowledge, only two examples of the derivatization of a polysaccharide with phosphorous-containing ester moieties have been reported to use microwave rather than conventional heating techniques, in order to provide a more efficient reaction. Indeed, microwave irradiation is well known in modern organic chemistry to provide a highly efficient form of heating, allowing for energy to be directly absorbed by the reactants, thus affording significantly higher reaction rates and product yields and selectivities [32]. The advantages of microwave irradiation have already been demonstrated for several reactions in the field of chemical modification of polysaccharide structures [33–35]. The two reports on microwave-assisted reactions of a polysaccharide with reacting phosphorous species regarded cellulose and levan. Cellulose was derivatized with phosphite groups with an almost quantitative DP, which was considerably higher and faster achieved with respect to the phosphite-derivatized cellulose obtained by conventional heating [36]. Similarly, levan was functionalized with phosphate monoester groups under microwave irradiation with a higher DP with respect to conventional heating [37].

Since we have very recently started to screen different phosphorylating reagents towards the semi-synthesis of regioselectively phosphorylated chondroitin polysaccharide [27], starting from a microbial-sourced, unsulfated chondroitin (CS-0, 42 ± 3 KDa, 1.34 dispersity) derived from the fed-batch fermentation of *Escherichia coli* O5:K4:H4 [38], we have now focused our efforts on the optimization of the DP for the semi-synthesis of chondroitin 6-phosphate (CP-C) by applying microwave irradiation for the phosphorylation reaction. All the obtained CP samples have been characterized in detail, from both a structural and hydrodynamic point of view, highlighting the differences detected between the products obtained by microwave irradiation and standard heating protocol.

## 2. Materials and Methods

### *2.1. General Methods*

Commercial-grade reagents and solvents were used without further purification, except where differently indicated. The term "pure water" refers to water purified by a Millipore Milli-Q Gradient system (Millipore, Burlington, MA, USA). Microwave-irradiated reactions were performed with a CEM Discover 908010 instrument (CEM Corporation, Matthews, NC, USA). Dialyses were conducted on Spectra/Por 3.5 KDa cut-off membranes (Spectrum Labs, San Francisco, CA, USA) at 4 °C. Centrifugations were performed with an Eppendorf Centrifuge 5804R instrument (Eppendorf, Hamburg, Germany) at 4 °C (4600× *g*, 5 min). Sonications were performed with an Elmasonic S30H instrument (Elma Schmidbauer GmbH, Singen, Germany). Size-exclusion chromatography was performed on a Bio-Gel P4 column (0.75 × 67.5 cm, Bio-Rad, Hercules, CA, USA) using pure water as a buffer at a flow rate of 0.2 mL/min. Freeze-dryings were performed with a 5Pascal Lio 5P 4K freeze dryer (5Pascal, Milan, Italy). NMR spectra were recorded on a Bruker Avance-III HD ($^{1}$H: 400 MHz, $^{13}$C: 100 MHz, $^{31}$P: 162 MHz, Bruker, Billerica, MA, USA) or on a Bruker Avance-III ($^{1}$H: 600 MHz, $^{13}$C: 150 MHz, Bruker, Billerica, MA, USA) instrument—the latter equipped with a cryo-probe—in $D_2O$ (acetone as internal standard, $^{1}$H: $(CH_3)_2CO$ at δ 2.22; $^{13}$C:$(CH_3)_2CO$ at δ 31.5; $H_3PO_4$ as external standard, $^{31}$P: δ 0.0). A high-performance size-exclusion chromatography–triple detector array (HP-SEC-TDA) Viscotek TDA 305 instrument (Malvern Panalytical, Malvern, UK) was used for hydrodynamic analyses.

### *2.2. Typical Procedure for Phosphorylation Reaction*

Polysaccharide **2** [39] (41.9 mg, 67.5 μmol) was mixed with urea (637 mg, 10.6 mmol) and then treated with dry *N*,*N*-dimethylformamide (DMF, 1.3 mL) and 85% $H_3PO_4$ (109 μL) under Ar atmosphere. The suspension was stirred at 80–150 °C under conventional heating or microwave irradiation for 1–3 h. The resulting yellowish suspension was cooled to

room temperature, and then methanol (14 mL) was added to form a white precipitate. The mixture was cooled in a freezer, and then the precipitate was collected by centrifugation. The solid was dissolved in HPLC-grade $H_2O$ (4.0 mL; pH ~ 2) and treated under stirring with a few drops of aqueous 33% NaOH to neutral pH. The solution was dialyzed and freeze-dried to afford CP-C product (24.4 mg, 58% mass yield).

### *2.3. Enzymatic Depolymerization of CP-C-7*

A suspension of **CP-C-7** (20.4 mg) in a 0.15 M NaCl, 0.10 M NaOAc solution (1.0 mL) was buffered to pH = 5 by adding a drop of acetic acid. The mixture was incubated at 37 °C for 1 h, then a solution of bovine testicular hyaluronidase (BTH, 1.9 mg) in pure water (950 µL) was added. The production of oligosaccharide species was detected in progress by silica-gel thin-layer chromatography (TLC; eluent: 1:1:1:0.05 *v*/*v*/*v*/*v* *n*-butanol/ethanol/water/acetic acid). After incubating for 165 h at 37 °C, the reaction was quenched by heating it at 100 °C for 15 min. By successive cooling and freeze-drying, a white solid residue (33.3 mg) was obtained. It was dissolved in the minimum amount of water and purified by size-exclusion chromatography to give three fractions (**LMW-CP-C-a**, 4.9 mg; **LMW-CP-C-b**, 5.7 mg; **LMW-CP-C-c**, 2.6 mg).

### *2.4. NMR Analyses*

NMR samples were prepared by adding 600 µL $D_2O$ to approx. 6 mg of each polysaccharide product. After prolonged stirring and sonication at room temperature, the solid residue, if any, was removed, and experiments were performed on the resulting supernatant. Data were processed using the data analysis packages integrated with Bruker TopSpin® 4.0.5 software. The $^{31}$P-NMR spectra were obtained by typically accumulating 512 transients. The $^{1}$H- and $^{31}$P-1D-DOSY experiments were measured using a stimulated echo sequence with bipolar gradient pulses and one spoil gradient (stebpgp1s1d) with a diffusion time Δ of 100 ms, a gradient duration of 2 or 4 ms (for $^{1}$H- and $^{31}$P-1D-DOSY, respectively), and accumulating 64 or 2048 transients (for $^{1}$H- and $^{31}$P-1D-DOSY, respectively). The $^{1}$H,$^{13}$C-DEPT-HSQC experiments were measured in the $^{1}$H-detected mode via single-quantum coherence with proton decoupling in the $^{13}$C domain, using data sets of 2048 × 256 points and typically 64 increments. The $^{1}$H,$^{31}$P-HSQC experiments were measured in the $^{1}$H-detected mode via phase-sensitive gradient selection with decoupling during acquisition, using a data set of 2048 × 256 points and typically 64 increments.

### *2.5. Hydrodynamic Analyses*

A comprehensive description of the HP-SEC-TDA Viscotek TDA 305 apparatus, employed for the hydrodynamic characterization of the samples, and its capabilities is reported elsewhere [40]. In brief, the instrumentation comprised two primary units: (i) the GPC-max VE 2001 integrated system (Malvern Panalytical, Malvern, UK), which includes a gel-permeation chromatography pump, an in-line solvent degasser, and an autosampler; (ii) the TDA302 triple detector array module (Malvern Panalytical, Malvern, UK), equipped with a column oven, a refractive index (RI) detector, a viscometer, as well as right-angle (RALS) and low-angle (LALS) light scattering detectors. The light scattering detectors were optimized to maximize the signal-to-noise ratio, with measurements taken at a 7° angle relative to the incident beam. Two TSK–GEL GMPWXL columns (Tosoh Bioscience, Tokyo, Japan; Cat. No. 8-08025; hydroxylated polymethacrylate, pore size—100–1000 Å, particle size—13 µm, dimensions—7.8 × 30.0 cm) were connected in series, preceded by a guard column (Tosoh Bioscience; Cat. No. 08033; particle size—12 µm, 6.0 × 4.0 cm).

Samples were dissolved/dispersed in deionized water to a concentration of approximately 10 mg/mL, followed by appropriate dilution for analysis (final column load ranging between 0.2 and 0.4 dL). Prior to injection, all samples were filtered using disposable 0.22 µm syringe filters. Chromatographic analyses were carried out under isocratic condi-

tions employing a 0.1 M aqueous $NaNO_3$ solution (pH 7.0) as the mobile phase, at a flow rate of 0.6 mL/min and a column temperature of 40 °C, with a total runtime of one hour. Data acquisition and processing were performed using OmniSEC software 11.36 (Malvern Instruments, Malvern, UK). A dn/dc value of 0.155 mL/g was applied for calculations. The determined parameters included weight-average molecular weight ($M_w$), number-average molecular weight ($M_n$), polydispersity index ($M_w/M_n$), hydrodynamic radius ($R_h$), and intrinsic viscosity ([η]). Additionally, the sample fraction/wt% having a molecular weight above 20 KDa was derived.

## 3. Results and Discussion

A screening of phosphorylation conditions performed on the *n*-tetrabutylammonium salt of *E. coli* sourced CS-0 (**2** [39], Scheme 1) was very recently reported by us [27]. CP-C could be obtained by a conventional heating reaction either with PEP-K and TBAHS at 80 °C for 48 h, achieving a DP-6 (degree of phosphorylation at GalNAc O-6 site) of 0.36 or with $H_3PO_4$ in DMF at 120 °C for 3 h in the presence of urea to give a DP-6 of 0.49. The latter result (Table 1, entry 1) was selected as the best starting point to perform a screening of microwave irradiation conditions for the same phosphorylation method in order to increase the DP-6. Lower reaction time (2 h) and temperature (80 °C) with respect to conventional heating were initially tested to give **CP-C-2** product (Table 1, entry 2), after *n*-tetrabutylammonium/$Na^+$ exchange and purification by dialysis. No derivatization was achieved under these conditions, as detected by comparing $^1$H-NMR spectra of **CP-C-1** and starting CS-0 (Figure S1 in Supplementary Materials).

**Table 1.** Phosphorylation tests on **2** with $H_3PO_4$, urea, and DMF under different reaction conditions.

| Entry | Product | Conditions | Mass Yield | DP-6 [a] | $^{31}$P Signals [b] |
|---|---|---|---|---|---|
| 1 | **CP-C-1** [c] | Conventional heating: 120 °C, 3 h | 74% | 0.49 | 0.7 |
| 2 | **CP-C-2** | Microwave irradiation: 80 °C, 1 h, 13 W, 20 psi | 56% | 0 | -- |
| 3 | **CP-C-3** | Microwave irradiation: 100 °C, 1 h, 50 W, 50 psi | 51% | 0.12 | 2.6 |
| 4 | **CP-C-4** | Microwave irradiation: 120 °C, 1 h, 100 W, 50 psi | 79% | 0.20 | 2.4 |
| 5 | **CP-C-5** | Microwave irradiation: 120 °C, 1 h, 100 W, 300 psi | 66% | 0.27 | 2.5 |
| 6 | **CP-C-6** | Microwave irradiation: 120 °C, 3 h, 100 W, 300 psi | 58% | 0.83 | 3.4, −5.9, −10.0 |
| 7 | **CP-C-7** | Conventional heating: 120 °C, 3 h (twice) | 56% | 0.51 | 3.9 |
| 8 | **CP-C-8** | Conventional heating: 150 °C, 3 h | 69% | 1.00 | 2.0, −0.4, −7.0, −10.5, −11.2, −20.0 |

[a] Degree of phosphorylation at GalNAc O-6 site, measured by relative integration of $CH_2$ signal at 3.92/64.5 and 3.75/62.3 ppm assigned to GalNAc-6 phosphate and GalNAc $CH_2$-6, respectively, in the $^1$H,$^{13}$C-DEPT-HSQC 2D-NMR spectrum (Figure 2a,c and Figures S3–S9). [b] Chemical shift values measured by $^{31}$P-DOSY 1D-NMR spectrum. [c] See [27].

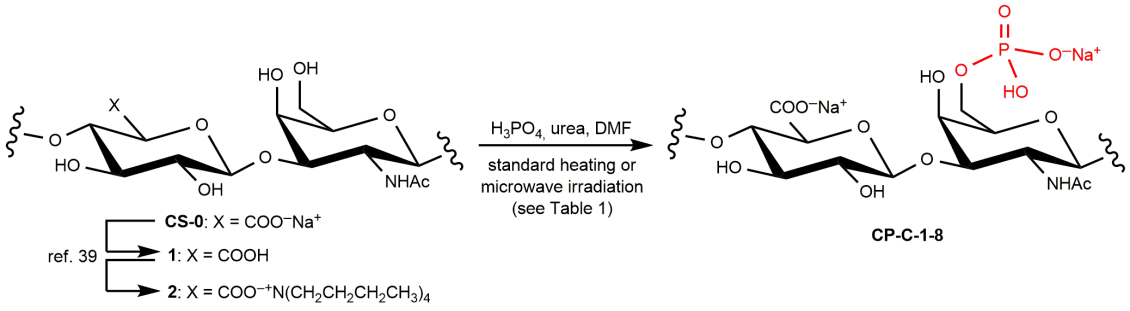


**Scheme 1.** Regioselective phosphorylation of *E. coli*-sourced chondroitin to CP-C (phosphate group in red).

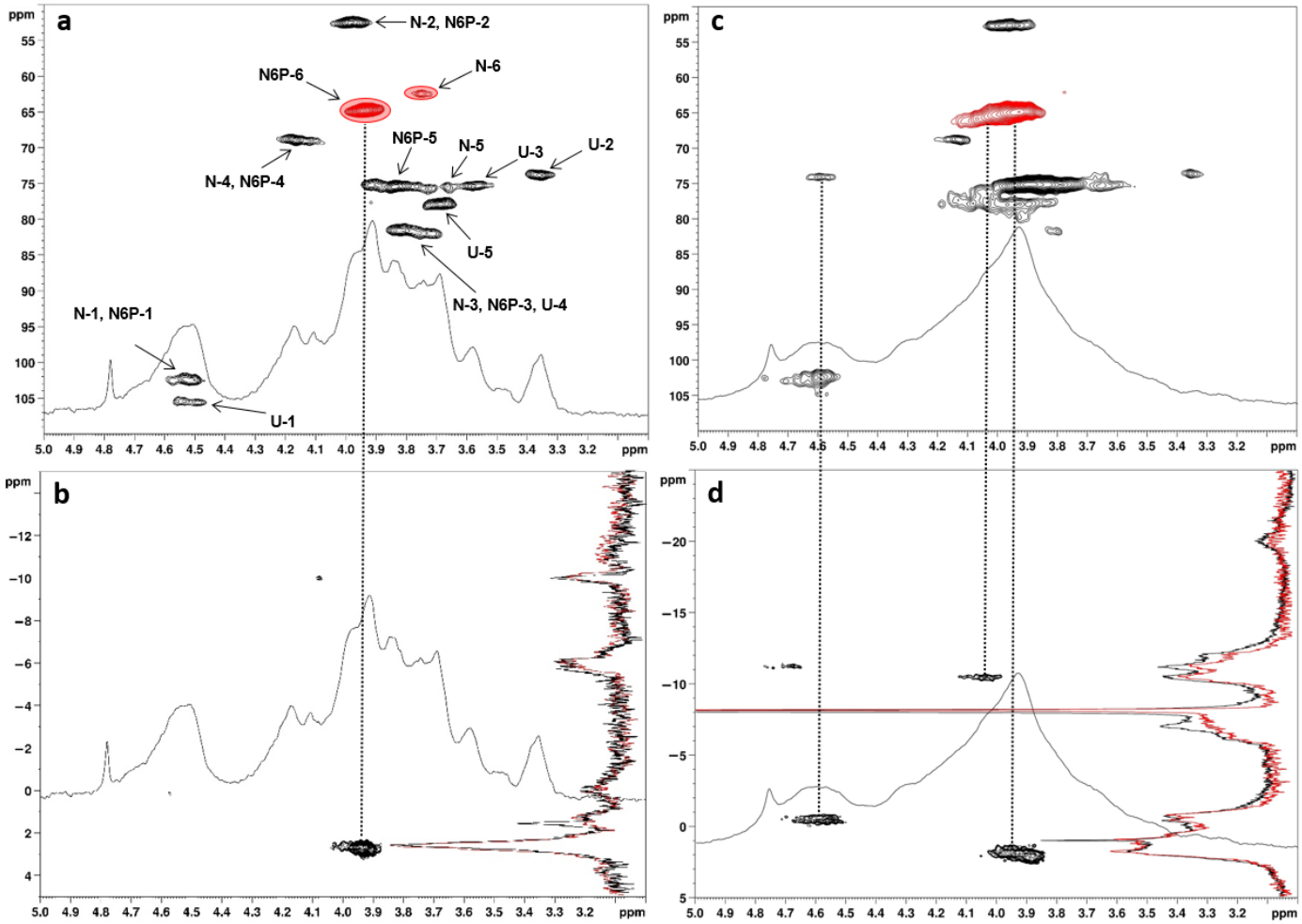


**Figure 2.** Superimposed, zoomed $^{1}$H and $^{1}$H,$^{13}$C-DEPT-HSQC (**a**,**c**) and $^{1}$H, $^{31}$P, $^{31}$P-1D-DOSY (in red) and $^{1}$H,$^{31}$P-HSQC (**b**,**d**) NMR spectra ($D_2O$, 400 MHz, 298 K) of **CP-C-6** (**a**,**b**) and **CP-C-8** (**c**,**d**) (N—GalNAc, N6P—GalNAc-6-phosphate, U—GlcA; densities enclosed in red circles were integrated for DP-6 estimation).

Under stronger microwave irradiating conditions (Table 1, entry 3), the regioselective installation of the phosphate group at GalNAc *O*-6 site could be achieved, as confirmed by a set of both 1D- and 2D-NMR experiments. The former set comprised $^{1}$H-NMR, $^{31}$P-NMR, and $^{31}$P-1D-DOSY spectra (the last one being fundamental to discriminate between phosphorus-containing moieties either covalently linked to the chondroitin polysaccharide or present in small molecule impurities such as inorganic phosphate or diphosphate), while the $^{1}$H,$^{31}$P-HSQC and $^{1}$H,$^{13}$C-DEPT-HSQC sequences were employed for 2D-NMR measurements. In particular, the latter 2D-NMR spectrum of **CP-C-3** showed two small signals sensibly shifted to different chemical shift values with respect to starting CS-0, at $\delta_{H/C}$ 3.77/73.6 and 3.92/64.5 (Figure S2 in Supplementary Materials). These could be assigned to CH-5 and $CH_2$-6 atoms of GalNAc-6-phosphate units, respectively, by comparison with values from the literature [27] and also by detecting the signal at $\delta_{H/P}$ 3.92/2.6 in the $^{1}$H,$^{31}$P-HSQC 2D-NMR spectrum of **CP-C-3** (Figure S3 in Supplementary Materials). By assuming that the signals at $\delta_{H/C}$ 3.92/64.5 and 3.76/62.4—assigned to $CH_2$-6 atoms of GalNAc-6-phosphate and underivatized GalNAc units, respectively—displayed similar $^{1}J_{C,H}$ coupling constants and that a difference of around 5–8 Hz from the experimental set value could not cause a substantial variation in the integrated peak volumes [41], their relative integration returned a DP-6 equal to only 0.12 for **CP-C-3**. In order to increase it, the microwave phosphorylation was conducted under even stronger

irradiating conditions (Table 1, entries 4–6). Finally, the $^{1}H,^{13}C$-DEPT-HSQC 2D-NMR spectrum of the **CP-C-6** sample (Figure 2a), which was obtained by reacting **2** for 3 h at 120 °C under 100 W microwave irradiation at 300 psi, showed a DP-6 equal to 0.83 without impairing the GalNAc O-6 regioselectivity. This value was considerably higher with respect to the DP-6 resulting from the reaction conducted under the same conditions but with standard heating (0.49 for **CP-C-1**) [27]. It bears noting that the attempt to further increase the latter by repeating the reaction twice gave a negligible enhancement of DP-6 (0.51; Table 1, entry 7), while an increase in temperature to 150 °C (Table 1, entry 8) afforded the **CP-C-8** product with a quantitative DP-6 but a decreased regioselectivity. Indeed, its $^{1}H,^{13}C$-DEPT-HSQC 2D-NMR spectrum showed a remarkably downfield-shifted CH signal at $\delta_{H/C}$ 4.60/73.9 (Figure 2c), which could be associated with the phosphorylation of secondary hydroxyls by the cross-peak at $\delta_{H/P}$ 4.60/−0.4 in the $^{1}H,^{31}P$-HSQC 2D-NMR spectrum (Figure 2d). The order of reactivity of the secondary hydroxyls of chondroitin polysaccharide is known to have the OH at the C-2 atom of GlcA units as the most reactive one under sulfation conditions [42]. Unfortunately, the collected 2D-NMR spectra of **CP-C-8** were not able to confirm or discard this trend, plausibly due to a too heterogeneous structure hampering a clear attribution of the signals.

Indeed, the higher structural heterogeneity of the **CP-C-8** sample was related not only to the presence of multiple phosphorylation sites but also to the detection of peaks in different regions of its $^{31}P$ and $^{31}P$-1D-DOSY spectra. Indeed, together with broad peaks at 2.0 and −0.4 ppm assigned to monophosphate groups at the two different derivatization positions, some additional signals of similar intensity were detected at −7.0, −10.5, and −11.2 ppm. These could be due to the presence of some diphosphate groups decorating the chondroitin backbone, as clearly evidenced by the $^{1}H,^{31}P$-HSQC 2D-NMR spectrum of **CP-C-8** (Figure 2d), showing cross-peaks at $\delta_{H/P}$ 4.06/−10.5 and 4.62/−11.2. In particular, these signals could be assigned to the phosphorus atoms of diphosphate groups directly attached at GalNAc O-6 and at a secondary hydroxyl site, respectively (α-phosphorus atoms), while the $^{31}P$-signal at −7.0 ppm, that was not correlated to any $^{1}H$ signal in the $^{1}H,^{31}P$-HSQC 2D-NMR spectrum, could be assigned to the distal phosphorus atoms of both diphosphate groups (β-phosphorus atoms) [43,44]. A minor amount of triphosphate groups decorating the chondroitin backbone could also be inferred by the less intense $^{31}P$ signal at −20.0 ppm, which could be assigned to their middle β-phosphorus atoms, being the α- and γ-ones (closest and farthest to the attachment site on the polysaccharide backbone, respectively) overlapped with the α- and β-phosphorus signals of diphosphate groups [43]. Interestingly, the presence of signals associated with diphosphate groups could also be detected in the **CP-C-6** product from microwave irradiated phosphorylation, although in a much lower amount with respect to **CP-C-8**. It bears noting that, even if the presence of cyclic 4,6-phosphate diesters on *galacto*-configured sugars was sometimes reported in natural polysaccharides from bacterial membranes [45,46], this structural feature could be ruled out in the **CP-C-8** case. Indeed, it would have required a correlation in the $^{1}H,^{31}P$-HSQC 2D-NMR spectrum between a single $^{31}P$-chemical shift with two different $^{1}H$-chemical shifts, assignable through the $^{1}H,^{13}C$-DEPT-HSQC spectrum to a CH- and a $CH_2$-type signal, respectively. This was not observed in the reported 2D-NMR spectra.

In parallel with the structural characterization by NMR, some hydrodynamic parameters were also determined for phosphorylated polysaccharides **CP-C-3-8** by HP-SEC-TDA analysis (Table 2). For all the products obtained by phosphorylation under microwave irradiation (**CP-C-3-6**) a lower weight-average molecular weight was detected with respect to the starting polysaccharide **CS-0** (Table 2, entry 1, 37 KDa), as expected for the acid character—although weak—of the employed phosphorylating agent ($H_3PO_4$), triggering the cleavage of some of the glycosidic bonds connecting the monose residues in the polysac-

charide chain. Moreover, with the gradual increase in the strength of microwave irradiating conditions from **CP-C-3** to **CP-C-6**, a gradually more pronounced depolymerization was detected with the weight-average molecular weight value lowering from 27 KDa (**CP-C-3**, Table 2, entry 2) to 11 KDa (**CP-C-5**, Table 2, entry 4) and the sample fraction exceeding 20 KDa lowering from 65% (**CP-C-3**) to 10% (**CP-C-5**). It bears noting that the product **CP-C-6**, which was obtained under the same microwave conditions of **CP-C-5** but after a longer irradiation time (3 and 1 h, respectively), showed a slightly higher molecular weight (17 KDa, sample fraction with $M_w$ > 20 KDa = 14%; Table 2, entry 5) with respect to the latter. This could be first ascribed to the much higher DP-6 of **CP-C-6** with respect to **CP-C-5** (0.83 vs. 0.27: see Table 1, entries 5 and 6), accounting for a much more frequent and therefore much "heavier" decoration of the chondroitin backbone with phosphate and—to a lower extent—even diphosphate groups.

**Table 2.** Hydrodynamic parameters for **CS-0** starting material and phosphorylated polysaccharides **CP-C-3,8**.

| Entry | Product | Recovery [a] (wt%) | Peak Representativeness (wt%) | $M_w$ (kDa) | $M_w$ > 20 KDa Fraction (wt%) | $M_w/M_n$ | [η] (dL/g) |
|---|---|---|---|---|---|---|---|
| 1 | **CS-0** | 103 ± 6 | 100 | 37 ± 3 | 95 ± 8 | 1.12 ± 0.07 | 1.27 ± 0.06 |
| 2 | **CP-C-3** | 67 ± 5 | 91 ± 3 | 27 ± 2 | 65 ± 3 | 1.39 ± 0.05 | 0.82 ± 0.05 |
| 3 | **CP-C-4** | 68 ± 5 | 85 ± 6 | 13 ± 2 | 16 ± 1 | 1.40 ± 0.04 | 0.38 ± 0.05 |
| 4 | **CP-C-5** | 64 ± 4 | 92 ± 5 | 11 ± 1 | 10 ± 1 | 1.39 ± 0.02 | 0.30 ± 0.03 |
| 5 | **CP-C-6** | 51 ± 3 | 87 ± 6 | 18 ± 3 | 14 ± 1 | 3.3 ± 0.3 | 0.18 ± 0.02 |
| 6 | **CP-C-7** | 75 | 36 [b] | 23 | 30 | 1.95 | 0.37 |
| 7 | **CP-C-8** | 47 | 27<br>23<br>26<br>18<br>6 | 18<br>47<br>15<br>587<br>4000 | 37<br>100<br>100<br>100<br>100 | 2.08<br>1.09<br>1.16<br>1.24<br>1.26 | 0.088<br>0.093<br>0.21<br>0.49<br>1 |

[a] Weight recovery after centrifugation of a 7.5 mg/mL suspension of the product in pure water; [b] Data refer to only one of the two peaks detected by the RI detector; the second peak showed extremely low laser and viscometer signal intensity, thus failing to provide a molecular weight value and likely corresponding to inorganic phosphate species, as confirmed by comparison of $^{31}$P- and $^{31}$P-DOSY NMR spectra (see Figure S7 in Supplementary Materials).

A completely different result was observed for **CP-C-8**, as it showed a very large distribution of molecular weights, with four peaks of similar representativeness in the HP-SEC chromatogram spanning from 18 to hundreds of KDa and a fifth, minor one reaching even 4 MDa (Figures S12 and S13 in Supplementary Materials). The formation of such high-molecular-weight species could be ascribed to the presence of mono- and/or diphosphate diester moieties acting as cross-linkers between different polysaccharide chains. The cross-linking between polysaccharide chains through phosphodiester functionalities is not unprecedented, and includes also the case of a GAG polysaccharide, such as hyaluronic acid [47], although it has always been accomplished with the use of sodium trimetaphosphate rather than $H_3PO_4$ as the phosphorylation/cross-linking agent [48]. Cross-linking could occur through monophosphate and/or diphosphate diester. The formation of the latter in **CP-C-8** is not in disagreement with its $^{31}$P-NMR data. Diphosphate diesters typically give a signal at approx. −10 ppm that can be overlapped with peaks related to α-phosphorous atoms of diphosphate monoester moieties [43]. The $^{31}$P-NMR spectrum of **CP-C-8** indeed shows signals at such chemical shift values, as already discussed above (Figure 2d). Conversely, cross-linking through monophosphate diesters should be plausibly ruled out. Indeed, such moieties typically give $^{31}$P signals at approx. 0 ppm [43]. In spite of the $^{31}$P-NMR spectrum of **CP-C-8** showing a signal in such a chemical shift region, the

$^{1}$H,$^{31}$P-HSQC 2D-NMR spectrum allows for correlating it only with a single $^{1}$H chemical shift (Figure 2d), corresponding in turn to a CH-tagged density in the $^{1}$H,$^{13}$C-DEPT-HSQC 2D-NMR spectrum (Figure 2c). This would mean that the putative monophosphate diester cross-linking would bridge secondary hydroxyls placed at the same site in the two cross-linked chondroitin repeating units. This "symmetrical" cross-linking would be very unlikely not only from a statistical point of view, but also if one takes into consideration that primary hydroxyls are instead the most reactive sites towards phosphorylation, as theoretically expected and experimentally found in all the semi-synthesized derivatives, including **CP-C-8**.

Therefore, NMR analysis of **CP-C-8** supports the notion that the cross-linking reaction was really happening under the harshest phosphorylation conditions while employing a conventional heating protocol (150 °C, 3 h: Table 1, entry 8). It is important to note that any significant evidence of a cross-linking reaction could be found for all the other products (**CP-C-3-7**), neither by $^{31}$P-NMR spectroscopy (Figures S3–S7 in Supplementary Materials) nor by the presence of significantly represented peaks associated with high-molecular-weight species in the HP-SEC chromatogram (Figures S13 and S14 in Supplementary Materials). Nonetheless, a comparison of intrinsic viscosity vs. molecular weight relationships for the phosphorylated products obtained by microwave irradiation, or obtained by overlapping the Mark–Houwink–Sakurada plots for **CP-C-3-6** (Figure 3), clearly revealed a gradual increase in the compactness of the polysaccharide conformation in solution with the increase in DP-6 (Table 1, entries 1, 3–6). These observations could be explained by polymer chain cross-linking, although the amount of phosphodiester moieties acting to this aim is too low to be detected by $^{31}$P-NMR spectroscopy in the case of **CP-C-3-5,** or can be ascribed only to minor peaks in **CP-C-6**. The higher dispersity (Mw/Mn) of the latter with respect to **CP-C-3-5** derivatives concurred to define the same trend in the increasing degree of cross-linking. Moreover, an additional clue that a cross-linking reaction could happen, not only for **CP-C-8** but also during the reactions giving products **CP-C-3-7**, comes from their lower water solubility with respect to the starting **CS-0** polysaccharide. Indeed, the weight recovery after centrifugation of a 7.5 mg/mL suspension in pure water is quantitative for **CS-0**, while it spans from 47% to around 70% for the phosphorylated polysaccharides, the lower being associated with the **CP-C-8** product, for which the HP-SEC-TDA analysis of the soluble fraction revealed an extensive cross-linking, as discussed above. The analysis of the structural features of the water-insoluble fractions could obviously be performed either by liquid-state NMR spectroscopy or by HP-SEC-TDA. It would require solid-state NMR techniques that are unfortunately not included among our current analytical facilities. Collaborative work with other research groups is being planned to tackle this issue. The results will be published as soon as possible elsewhere.

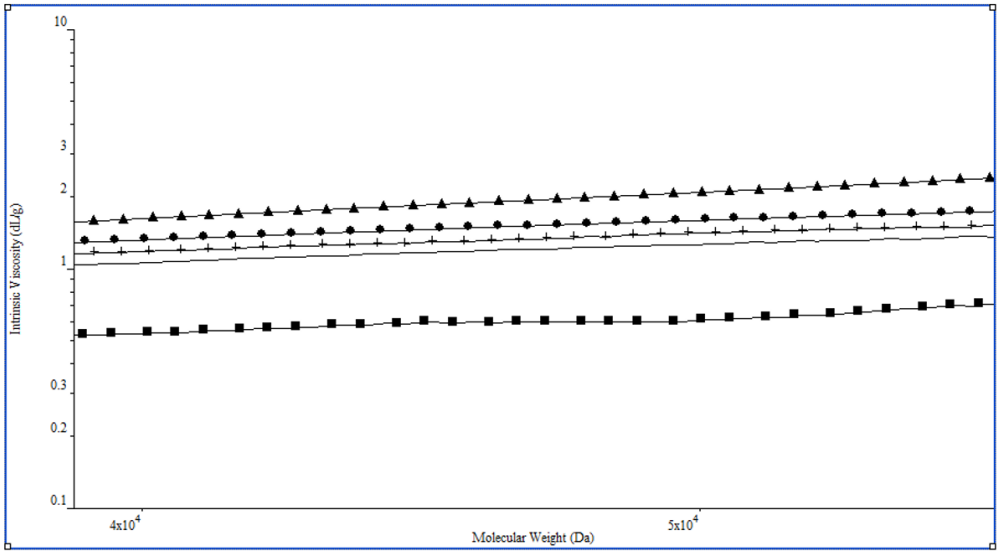


**Figure 3.** Overlap of the Mark–Houwink–Sakurada plots (intrinsic viscosity vs. $M_w$) for **CS-0** (solid triangle), **CP-C-3** (solid circle), **CP-C-4** (cross), **CP-C-5** (line, no style), and **CP-C-6** (solid square).

Successfully obtaining regioselectively phosphorylated CP-C derivatives prompted a preliminary study of their behavior in the presence of BTH, an endonuclease enzyme known for catalyzing the hydrolysis of hyaluronic acid, including some very recently reported, randomly phosphorylated derivatives thereof [49], and showing activity towards chondroitin and CS polysaccharides too [50]. The aim was not only to test the biodegradability of the obtained CP-C polysaccharides but also to open a direct access to low-molecular-weight species, i.e., CP oligosaccharides, that, to the best of our knowledge, are completely missing in the literature. It bears noting that several studies have demonstrated that low-molecular-weight chondroitin sulfate (LMW-CS) species have enhanced bioavailability and biological activities, including antioxidant, anticoagulation, anti-inflammatory, and neuroprotective effects, together with a safer profile in terms of absence of immunological responses [51,52]. Therefore, a future evaluation of LMW-CP-C biological properties would surely be worth pursuing. By incubating **CP-C-7** with BTH in a NaOAc/AcOH buffer (pH = 5) at 37 °C [53], three low-molecular-weight chondroitin phosphate species (named **LMW-CP-C-a**, **LMW-CP-C-b**, and **LMW-CP-C-c**, respectively) could be obtained after purification of the crude reaction mixture by size-exclusion chromatography. Their characterization by $^{1}$H- and $^{31}$P-1D-NMR as well as $^{1}$H,$^{13}$C-DEPT-HSQC- and $^{1}$H,$^{31}$P-HSQC-2D-NMR confirmed a structure of LMW chondroitin species carrying phosphate groups at some of GalNAc O-6 sites. In particular, a comparison of **CP-C-7** and **LMW-CP-C-a-c** $^{1}$H-NMR spectra clearly showed the presence of doublet signals at 5.13 and 4.59 ppm only in the latter case (Figure 4).

Since these signals corresponded in the $^{1}$H,$^{13}$C-DEPT-HSQC spectra to cross-peaks at $\delta_C$ 92.3 and 96.2, respectively, they could be assigned to the anomeric H atom of α- and β-configured GalNAc-reducing end units, respectively. A comparison between the sum of their integral values and the area of the signal at 1.94 ppm related to the methyl group of (reducing and non-reducing) GalNAc units through Equation (1), gave an estimation of the average chain length in the three LMW-CP samples: **LMW-CP-C-a** length distribution could be centered on a 23-mer species, while **LMW-CP-C-b** and **LMW-CP-C-c** could be estimated to be shorter (13-mer and 9-mer, respectively).

$$\text{average chain length} = [I(CH_3) \,/\, 3] \,/\, [I(\alpha\text{-reducing}) + I(\beta\text{-reducing})] * 2 \quad (1)$$

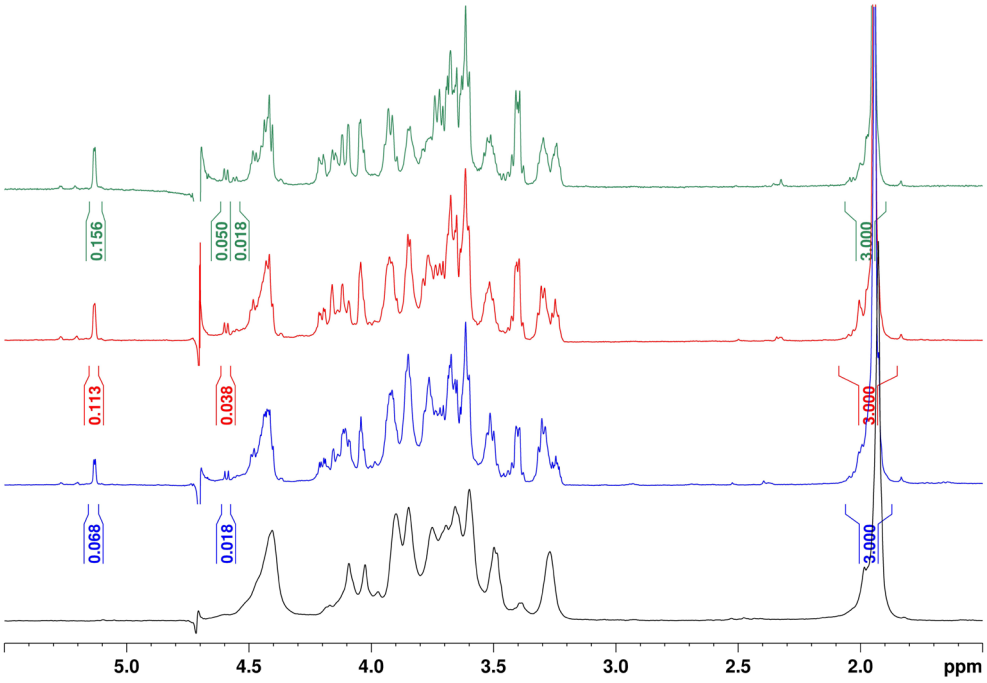


**Figure 4.** $^{1}$H NMR spectra ($D_2O$, 600 MHz, 298 K) of **CP-C-7** (black), **LMW-CP-C-a** (blue), **LMW-CP-C-b** (red), and **LMW-CP-C-c** (green).

By using the same equation, we could also compare the kinetic rate of BTH depolymerization for the **CP-C-7** sample and the starting chondroitin polysaccharide CS-0. From the $^{1}$H-NMR spectrum of the crude digest of the former (Figure S9 in Supplementary Materials), a length distribution centered on a 14-mer species was found, in agreement with the values indicated above for the fractions derived thereof (9-mer to 23-mer). Native CS-0 enzymatic degradation under the same conditions furnished a length distribution of the obtained oligomers in the crude reaction mixture centered on a 5-mer species. By considering that the starting $M_w$ of CS-0 was approximately double with respect to **CP-C-7** (42 vs. 23 KDa), it was possible to estimate an approx. 6-fold higher rate of degradation for the natural polysaccharide with respect to its phosphorylated derivative **CP-C-7**.

Finally, the presence of GalNAc-6-phosphate units within **LMW-CP-C-a-c** structures was confirmed by the presence of a signal at $\delta_{H/P}$ 3.84/3.9 in their $^{1}$H,$^{31}$P-HSQC 2D-NMR spectra, corresponding to a $^{1}$H- and $^{13}$C-downfield-shifted $CH_2$ signal at $\delta_{H/C}$ 3.84/63.0 in their $^{1}$H,$^{13}$C-DEPT-HSQC spectra (Figures S10–S12 in Supplementary Materials).

## 4. Conclusions

The phosphorylation reaction of a microbial-sourced, unsulfated chondroitin polysaccharide with phosphoric acid was tested under different microwave irradiation and conventional heating conditions in order to semi-synthesize a phosphorylated mimic of one of the most commonly found chondroitin sulfate variants (CS-C), i.e., chondroitin-6-phosphate (CP-C). The collected products were subjected to a detailed characterization, in terms of chemical structure and hydrodynamic properties, by 1D- and 2D-NMR spectroscopy and HP-SEC-TDA analysis, respectively. The best result in terms of regioselectivity and degree of phosphorylation was achieved by microwave irradiation of the CS-0 starting material at 120 °C for 3 h. Under similar conditions, the application of a conventional heating protocol gave a lower DP-6, while the increase in the temperature enhanced the degree of derivatization but was detrimental for the regioselectivity and extensively triggered alternative reaction pathways, giving the formation of phosphate diester functionalities as cross-linkers between polysaccharide chains. The results from the screening presented

in this work could be of a certain interest for any research devoted to the regioselective phosphorylation of a polysaccharide. Moreover, the obtained CP-C polysaccharides, as well as their enzymatically derived LMW counterparts, that were already obtained in this work from the former, will be subjected in the near future to a comparison of their structural features and, above all, of their biological properties with the sulfated CS-C counterparts. The results of such an investigation will be published as soon as possible elsewhere. Last but not least, the present study represents an additional reference—even if the generalizability of results across different microwave equipment is still to be proven—in the growing field of microwave-assisted derivatizations of polysaccharides.

**Supplementary Materials:** The following supporting information can be downloaded at: https://www.mdpi.com/article/10.3390/polysaccharides7010011/s1, Figure S1: $^{1}$H NMR spectra superimposition of **CP-C-2** and CS-0; Figure S2: $^{1}$H, 1D-DOSY and $^{1}$H,$^{13}$C-DEPT-HSQC NMR spectra superimposition of **CP-C-3** and CS-0; Figures S3–S8: (a) $^{1}$H, 1D-DOSY, $^{1}$H,$^{13}$C-DEPT-HSQC, and (b) $^{1}$H, $^{31}$P, $^{31}$P-1D-DOSY, $^{1}$H,$^{31}$P-HSQC NMR spectra of **CP-C-3-8**; Figure S9: $^{1}$H NMR spectra superimposition of crude BTH digest of CS-0 and **CP-C-7**; Figures S10–S12: (a) $^{1}$H, $^{1}$H,$^{13}$C-DEPT-HSQC and (b) $^{1}$H, $^{31}$P, $^{1}$H,$^{31}$P-HSQC NMR spectra of **LMW-CP-C-a-c**; Figures S13,S14: HP-SEC profiles (RI signal) for CS-0 and **CP-C-3-8**.

**Author Contributions:** Conceptualization, F.E., S.T., A.I., and E.B.; methodology, F.E., A.L.G., and E.B.; investigation, F.E. and S.C.; data curation, F.E., S.C., A.L.G., and E.B.; writing—original draft preparation, A.L.G. and E.B.; writing—review and editing, F.E., S.T., A.I., D.C., and C.S.; supervision, S.T., D.C., A.L.G., and E.B.; funding acquisition, A.L.G., C.S., and E.B. All authors have read and agreed to the published version of the manuscript.

**Funding:** This research was funded by the Italian Ministry of Enterprises and Made in Italy (MIMIT, CROSSGAG project, CUP: B69J24001940005) and the Italian Ministry of University and Research (MUR, HealHyal project, CUP: E53D23020320001).

**Data Availability Statement:** The original contributions presented in this study are included in the article/Supplementary Materials. Further inquiries can be directed to the corresponding author.

**Conflicts of Interest:** The authors declare no conflicts of interest.

## Abbreviations

The following abbreviations are used in this manuscript:

| | |
|---|---|
| CS | Chondroitin sulfate |
| GAG | Glycosaminoglycans |
| GalNAc | *N*-acetyl-D-galactosamine |
| GlcA | D-glucuronic acid |
| DP | Degree of phosphorylation |
| DP-6 | Degree of phosphorylation at *N*-acetyl-D-galactosamine O-6 site |
| CS-0 | Unsulfated chondroitin |
| CP-C | Chondroitin 6-phosphate |
| NMR | Nuclear magnetic resonance |
| HP-SEC | High-performance size exclusion chromatography |
| TDA | Triple detector array |
| DMF | *N*,*N*-dimethylformamide |
| HPLC | High-performance liquid chromatography |
| NaOAc | Sodium acetate |
| AcOH | Acetic acid |

| | |
|---|---|
| BTH | Bovine testicular hyaluronidase |
| TLC | Thin-layer chromatography |
| LMW | Low molecular weight |
| DOSY | Diffusion-ordered spectroscopy |
| DEPT-HSQC | Distortionless enhancement by polarization transfer heteronuclear single-quantum correlation |
| RI | Refractive index |
| RALS | Right-angle light scattering |
| LALS | Low-angle light scattering |
| $M_w$ | Weight-average molecular weight |
| $R_h$ | Hydrodynamic radius |
| [η] | Intrinsic viscosity |
| $M_n$ | Number-average molecular weight |

## References


1. Bedini, E.; Corsaro, M.M.; Fernandez-Mayoralas, A.; Iadonisi, A. Chondroitin, dermatan, heparan, and keratan sulfate: Structure and functions. In *Extracellular Sugar-Based Biopolymers Matrices*; Cohen, E., Merzendorfer, H., Eds.; Springer Nature: Cham, Switzerland, 2019; pp. 187–223.
2. Ricard-Blum, S.; Vivès, R.R.; Schaefer, L.; Götte, M.; Merline, R.; Passi, A.; Heldin, P.; Magalhães, A.; Reis, C.A.; Skandalis, S.S.; et al. A biological guide to glycosaminoglycans: Current perspectives and pending questions. *FEBS J.* **2024**, *291*, 3331–3366. [CrossRef]
3. Collin, E.C.; Carroll, O.; Kilcoyne, M.; Peroglio, M.; See, E.; Hendig, D.; Alini, M.; Grad, S.; Pandit, A. Ageing affects chondroitin sulfates and their synthetic enzymes in the intervertebral disc. *Sig. Transduct. Target. Ther.* **2017**, *2*, 17049. [CrossRef] [PubMed]
4. Perez, S.; Makshakova, O.; Angulo, J.; Bedini, E.; Bisio, A.; de Paz, J.L.; Fadda, E.; Guerrini, M.; Hricovini, M.; Hricovini, M.; et al. Glycosaminoglycans: What remains to be deciphered? *J. Am. Chem. Soc. Au* **2023**, *3*, 628–656. [CrossRef] [PubMed]
5. Gama, C.I.; Tully, S.E.; Sotogaku, N.; Clark, P.M.; Rawat, M.; Vaidehi, N.; Goddard, W.A., III; Nishi, A.; Hsieh-Wilson, L.C. Sulfation patterns of glycosaminoglycans encode molecular recognition and activity. *Nat. Chem. Biol.* **2006**, *2*, 467–473. [CrossRef] [PubMed]
6. Swarup, V.P.; Hsiao, T.W.; Zhang, J.; Prestwich, G.D.; Kuberan, B.; Hlady, V. Exploiting differential surface display of chondroitin sulfate variants for directing neuronal outgrowth. *J. Am. Chem. Soc.* **2013**, *135*, 13488–13494. [CrossRef]
7. Miyata, S.; Komatsu, Y.; Yoshimura, Y.; Taya, C.; Kitagawa, H. Persistent cortical plasticity by upregulation of chondroitin 6-sulfation. *Nat. Neurosci.* **2012**, *15*, 414–422. [CrossRef]
8. Sugiura, N.; Clausen, T.M.; Shioiri, T.; Gustavsson, T.; Watanabe, H.; Salanti, A. Molecular dissection of placental malaria protein VAR2CSA interaction with a chemo-enzymatically synthesized chondroitin sulfate library. *Glycoconj. J.* **2016**, *33*, 985–994. [CrossRef]
9. Yu, Y.; Duan, J.; Leach, F.E., III; Toida, T.; Higashi, K.; Zhang, H.; Zhang, F.; Amster, I.J.; Linhardt, R.J. Sequencing the dermatan sulfate chain of decorin. *J. Am. Chem. Soc.* **2017**, *139*, 16986–16995. [CrossRef]
10. Ly, M.; Leach, F.E., III; Laremore, T.N.; Toida, T.; Amster, I.J.; Linhardt, R.J. The proteoglycan bikunin has a defined sequence. *Nat. Chem. Biol.* **2011**, *7*, 827–833. [CrossRef]
11. van Kuppevelt, T.H.; Oosterhof, A.; Versteeg, E.M.M.; Podhumljak, E.; van de Westerlo, E.M.A.; Daamen, W.F. Sequencing of glycosaminoglycans with potential to interrogate sequence-specific interactions. *Sci. Rep.* **2017**, *7*, 14785. [CrossRef]
12. Mende, M.; Bednarek, C.; Wawryszyn, M.; Sauter, P.; Biskup, M.B.; Schepers, U.; Bräse, S. Chemical synthesis of glycosaminoglycans. *Chem. Rev.* **2016**, *116*, 8193–8255. [CrossRef] [PubMed]
13. Zhang, X.; Lin, L.; Huang, H.; Linhardt, R.J. Chemoenzymatic synthesis of glycosaminoglycans. *Acc. Chem. Res.* **2020**, *53*, 335–346. [CrossRef] [PubMed]
14. Gottschalk, J.; Elling, L. Current state on the enzymatic synthesis of glycosaminoglycans. *Curr. Opin. Chem. Biol.* **2021**, *61*, 71–80. [CrossRef] [PubMed]
15. Badri, A.; Williams, A.; Awofiranye, A.; Datta, P.; Xia, K.; He, W.; Fraser, K.; Dordick, J.S.; Linhardt, R.J.; Koffas, M.A.G. Complete biosynthesis of a sulfated chondroitin in *Escherichia coli*. *Nat. Commun.* **2021**, *12*, 1389. [CrossRef]
16. Liu, K.; Guo, L.; Chen, X.; Liu, L.; Gao, C. Microbial synthesis of glycosaminoglycans and their oligosaccharides. *Trends Microbiol.* **2023**, *31*, 369–383. [CrossRef]
17. Restaino, O.F.; Schiraldi, C. Chondroitin sulfate: Are the purity and the structural features well assessed? A review on the analytical challenges. *Carbohydr. Polym.* **2022**, *292*, 119690. [CrossRef]
18. Zappe, A.; Miller, R.L.; Struwe, W.B.; Pagel, K. State-of-the-art glycosaminoglycan characterization. *Mass Spectrom. Rev.* **2022**, *41*, 1040–1071. [CrossRef]

19. Lane, R.S.; St. Ange, K.; Zolghadr, B.; Liu, X.; Schäffer, C.; Linhardt, R.J.; DeAngelis, P.L. Expanding glycosaminoglycan chemical space: Towards the creation of sulfated analogs, and novel and chimeric polymers. *Glycobiology* **2017**, *27*, 646–656. [CrossRef]
20. Vessella, G.; Traboni, S.; Cimini, D.; Iadonisi, A.; Schiraldi, C.; Bedini, E. Development of semisynthetic, regioselective pathways for accessing the missing sulfation patterns of chondroitin sulfate. *Biomacromolecules* **2019**, *20*, 3021–3030. [CrossRef]
21. Cimini, D.; Bedini, E.; Schiraldi, C. Biotechnological advances in the synthesis of modified chondroitin towards novel biomedical applications. *Biotechnol. Adv.* **2023**, *67*, 108185. [CrossRef]
22. Liu, Q.; Chen, G.; Chen, H. Chemical synthesis of glycosaminoglycan-mimetic polymers. *Polym. Chem.* **2019**, *10*, 164–171. [CrossRef]
23. Bojarski, K.K.; Becher, J.; Riemer, T.; Lemmnitzer, K.; Möller, S.; Schiller, J.; Schnabelrauch, M.; Samsonov, S.A. Synthesis and in silico characterization of artificially phosphorylated glycosaminoglycans. *J. Mol. Struct.* **2019**, *1197*, 401–416. [CrossRef]
24. Lima, M.A.; Rudd, T.R.; Fernig, D.G.; Yates, E.A. Phosphorylation and sulfation share a common biosynthetic pathway, but extend biochemical and evolutionary diversity of biological macromolecules in distinct ways. *J. R. Soc. Interface* **2022**, *19*, 20220391. [CrossRef] [PubMed]
25. Khaybrakhmanova, E.A.; Kozyrev, S.V.; Tyumkina, T.V.; Ponedel'kina, I.Y. Phosphorylation of hyaluronic acid. *Chem. Proc.* **2022**, *12*, 39. [CrossRef]
26. Uchimura, K.; Nishitsuji, K.; Chiu, L.-T.; Ohgita, T.; Saito, H.; Allain, F.; Gannedi, V.; Wong, C.-H.; Hung, S.-C. Design and synthesis of 6-O-phosphorylated heparan sulfate oligosaccharides to inhibit amyloid β-aggregation. *Chembiochem* **2022**, *23*, e202200191. [CrossRef]
27. Esposito, F.; Traboni, S.; Iadonisi, A.; Bedini, E. Towards the semi-synthesis of phosphorylated mimics of glycosaminoglycans: Screening of methods for the regioselective phosphorylation of chondroitin. *Carbohydr. Polym.* **2024**, *324*, 121517. [CrossRef]
28. Illy, N.; Fache, M.; Ménard, R.; Negrell, C.; Caillol, S.; David, G. Phosphorylation of bio-based compounds: The state of the art. *Polym. Chem.* **2015**, *6*, 6257–6291. [CrossRef]
29. Laffargue, T.; Moulis, C.; Remaud-Siméon, M. Phosphorylated polysaccharides: Applications, natural abundance, and new-to-nature structures generated by chemical and enzymatic functionalization. *Biotech. Adv.* **2023**, *65*, 108140. [CrossRef]
30. Wang, N.; Kong, Y.; Li, J.; Hu, Y.; Li, X.; Jiang, S.; Dong, C. Synthesis and application of phosphorylated saccharides in researching carbohydrate-based drugs. *Bioorg. Med. Chem.* **2022**, *68*, 116806. [CrossRef]
31. Zhou, S.; Huang, G. Preparation, structure and activity of polysaccharide phosphate esters. *Biomed. Pharmacother.* **2021**, *144*, 112332. [CrossRef]
32. Dudley, G.B.; Richert, R.; Stiegman, A.E. On the existence of and mechanism for microwave-specific reaction rate enhancement. *Chem. Sci.* **2015**, *6*, 2144–2152. [CrossRef]
33. Desbrières, J.; Petit, C.; Reynaud, S. Microwave-assisted modifications of polysaccharides. *Pure Appl. Chem.* **2014**, *86*, 1695–1706. [CrossRef]
34. Chen, X.; Yang, J.; Shen, M.; Chen, Y.; Yu, Q.; Xie, J. Structure, function and advance application of microwave-treated polysaccharide: A review. *Trends Food Sci. Technol.* **2022**, *123*, 198–209. [CrossRef]
35. Verdoliva, V.; Bedini, E.; De Luca, S. Sustainable chemical modification of natural polysaccharides: Mechanochemical, solvent-free conjugation of pectins and hyaluronic acid promoted by microwave radiations. *Biomacromolecules* **2024**, *25*, 6217–6228. [CrossRef]
36. Gospodinova, N.; Grelard, A.; Jeannin, M.; Chitanu, G.C.; Carpov, A.; Thiéry, V.; Besson, T. Efficient solvent-free microwave phosphorylation of microcrystalline cellulose. *Green Chem.* **2002**, *4*, 220–222. [CrossRef]
37. Huang, T.-Y.; Huang, M.-Y.; Tsai, C.-K.; Su, W.-T. Phosphorylation of levan by microwave-assisted synthesis enhanced anticancer ability. *J. Biosci. Bioeng.* **2021**, *131*, 98–106. [CrossRef]
38. Cimini, D.; Restaino, O.F.; Schiraldi, C. Microbial production and metabolic engineering of chondroitin and chondroitin sulfate. *Emerg. Top. Life Sci.* **2018**, *2*, 349–361. [CrossRef]
39. Vessella, G.; Vázquez, J.A.; Valcárcel, J.; Lagartera, L.; Monterrey, D.T.; Bastida, A.; García-Junceda, E.; Bedini, E.; Fernández-Mayoralas, A.; Revuelta, J. Deciphering structural determinants in chondroitin sulfate binding to FGF-2: Paving the way to enhanced predictability of their biological functions. *Polymers* **2021**, *13*, 313. [CrossRef]
40. La Gatta, A.; De Rosa, M.; Marzaioli, I.; Busico, T.; Schiraldi, C. A complete hyaluronan hydrodynamic characterization using a size exclusion chromatography-triple detector array system during in vitro enzymatic degradation. *Carbohydr. Polym.* **2010**, *404*, 21–29. [CrossRef]
41. Guerrini, M.; Naggi, A.; Guglieri, S.; Santarsiero, R.; Torri, G. Complex glycosaminoglycans: Profiling substitution patterns by two-dimensional nuclear magnetic resonance spectroscopy. *Anal. Biochem.* **2005**, *337*, 35–47. [CrossRef]
42. Bedini, E.; Laezza, A.; Iadonisi, A. Chemical Derivatization of sulfated glycosaminoglycans. *Eur. J. Org. Chem.* **2016**, *2016*, 3018–3042. [CrossRef]
43. Zhao, M.; Fujisawa, S.; Saito, T. Distribution and quantification of diverse functional groups on phosphorylated nanocellulose surfaces. *Biomacromolecules* **2021**, *22*, 5214–5222. [CrossRef] [PubMed]

44. Ponedel'kina, I.Y.; Khaibrakhmanova, E.A.; Kozyrev, S.V.; Tyumkina, T.V. Solid-phase phosphorylation of polysaccharides by phosphorus pentoxide. *Chem. Nat. Compd.* **2023**, *59*, 625–628. [CrossRef]
45. Cox, A.D.; Perry, M.B. Structural analysis of the O-antigen-core region of the lipopolysaccharide from *Vibrio cholerae* O139. *Carbohydr. Res.* **1996**, *290*, 59–65. [CrossRef]
46. Senchenkova, S.N.; Zatonsky, G.V.; Shashkov, A.S.; Knirel, Y.A.; Jansson, P.E.; Weintraub, A.; Albert, M.J. Structure of the O-antigen of *Vibrio cholerae* O155 that shares a putative D-galactose 4,6-cyclophosphate-associated epitope with *V. cholerae* O139 Bengal. *Eur. J. Biochem.* **1998**, *254*, 58–62. [CrossRef]
47. Dulong, V.; Lack, S.; Le Cerf, D.; Picton, L.; Vannier, J.P.; Miller, G. Hyaluronan-based hydrogels particles prepared by crosslinking with trisodium trimetaphosphate. Synthesis and characterization. *Carbohydr. Polym.* **2004**, *57*, 1–6. [CrossRef]
48. Carvalho Alavarse, A.; Garcia Frachini, E.C.; Cruz Gomes da Silva, R.L.; Hashimoto Lima, V.; Shavandi, A.; Freitas Siqueira Petri, D. Crosslinkers for polysaccharides and proteins: Synthesis conditions, mechanisms, and crosslinking efficiency, a review. *Int. J. Biol. Macromol.* **2022**, *202*, 558–596. [CrossRef]
49. Khaibrakhmanova, E.A.; Kozyrev, S.V.; Ponedel'kina, I.Y. In vitro biodegradability of phosphorylated hyaluronic acid by testicular hyaluronidase. *Chem. Proc.* **2023**, *14*, 75. [CrossRef]
50. Wang, K.; Qi, L.; Zhao, L.; Liu, J.; Guo, Y.; Zhang, C. Degradation of chondroitin sulfate: Mechanism of degradation, influence factors, structure-bioactivity relationship and application. *Carbohydr. Polym.* **2023**, *301*, 120361. [CrossRef]
51. Lan, R.; Li, Y.; Shen, R.; Yu, R.; Jing, L.; Guo, S. Preparation of low-molecular-weight chondroitin sulfates by complex enzyme hydrolysis and their antioxidant activities. *Carbohydr. Polym.* **2020**, *241*, 116302. [CrossRef]
52. Li, H.; Yuan, Q.; Lv, K.; Ma, H.; Gao, C.; Liu, Y.; Zhang, S.; Zhao, L. Low-molecular-weight fucosylated glycosaminoglycan and its oligosaccharides from sea cucumber as novel anticoagulants: A review. *Carbohydr. Polym.* **2021**, *251*, 117034. [CrossRef]
53. Kinoshita, A.; Yamada, S.; Haslam, S.M.; Morris, H.R.; Dell, A.; Sugahara, K. Isolation and structural determination of novel sulfated hexasaccharides from squid cartilage chondroitin sulfate E that exhibits neuroregulatory activities. *Biochemistry* **2001**, *40*, 12654–12665. [CrossRef]